Comprehensive phenotyping and transcriptome profiling to study nanotoxicity in *C. elegans*

Charles Viau[1,*], Orçun Haçariz[1,*], Farial Karimian[1] and Jianguo Xia[1,2]

[1] Institute of Parasitology, McGill University, Montreal, Canada
[2] Department of Animal Science, McGill University, Montreal, Quebec, Canada
[*] These authors contributed equally to this work.

ABSTRACT

Engineered nanoparticles are used at an increasing rate in both industry and medicine without fully understanding their impact on health and environment. The nematode *Caenorhabditis elegans* is a suitable model to study the toxic effects of nanoparticles as it is amenable to comprehensive phenotyping, such as locomotion, growth, neurotoxicity and reproduction. In this study, we systematically evaluated the effects of silver (Ag) and five metal oxide nanoparticles: SiO_2, CeO_2, CuO, Al_2O_3 and TiO_2. The results showed that Ag and SiO_2 exposures had the most toxic effects on locomotion velocity, growth and reproduction, whereas CeO_2, Al_2O_3 and CuO exposures were mostly neurotoxic. We further performed RNAseq to compare the gene expression profiles underlying Ag and SiO_2 toxicities. Gene set enrichment analyses revealed that exposures to Ag and SiO_2 consistently downregulated several biological processes (regulations in locomotion, reproductive process and cell growth) and pathways (neuroactive ligand-receptor interaction, wnt and MAPK signaling, etc.), with opposite effects on genes involved in innate immunity. Our results contribute to mechanistic insights into toxicity of Ag and SiO_2 nanoparticles and demonstrated that *C. elegans* as a valuable model for nanotoxicity assessment.

Subjects Bioinformatics, Molecular Biology, Toxicology, Ecotoxicology
Keywords *C. elegans*, Ag, SiO2, Nanoparticles, Locomotion Velocity, Growth Inhibition, Reproduction, Neurotoxicity, RNAseq

Submitted 10 October 2019
Accepted 4 February 2020
Published 27 February 2020

Corresponding author
Jianguo Xia, jeff.xia@mcgill.ca

Academic editor
Monika Mortimer

Additional Information and Declarations can be found on page 22

DOI **10.7717/peerj.8684**

INTRODUCTION

The use of engineered nanoparticles has increased enormously over the last decade, and the nanotechnology industry has grown from a 10-billion-dollar enterprise in 2012 to being valued over one trillion dollars in 2015 (*Gao et al., 2011*). However, the potential impacts of these nanoparticles on environment and animals have not been fully characterized and further research is warranted. Nanoparticles are defined as particulate matter ranging from 1 to 100 nm in size with properties not exhibited by their larger bulk counterparts (*Khanna et al., 2015*; *Capco & Chen, 2014*; *Maynard, 2011*; *Djurišić et al., 2015*). The reactivity of nanoparticles depends on their size, charge, dose as well as the chemical composition of their coating (*Medina et al., 2007*). For instance, the surface area of smaller nanoparticles

is larger compared to their larger counterparts, meaning they are more reactive and hence have a larger propensity of being toxic (*Oberdörster, 2010*).

Caenorhabditis elegans is a free-living soil nematode reaching approximately one millimeter in length in adult stage and has a relatively simple life cycle that can be grown on solid (i.e., nematode growth medium, NGM) or liquid media (i.e., S-medium) (*Brenner, 1974*; *Lewis & Fleming, 1995*). The small size and relatively cheap maintenance cycle of *C. elegans* make the nematode very amenable for various phenotype screening. *C. elegans* has been well-established as an *in vivo* model for testing the effects of heavy metals and novel anthelminthics (*Kaletta & Hengartner, 2006*; *Ruiz-Lancheros et al., 2011*). In terms of conservation of genes and biological pathways with humans, *C. elegans* shares 60 to 80% gene homology and possesses 12 of the 17 known signal transduction pathways (*Kaletta & Hengartner, 2006*; *National Research Council, 2000*).

To validate our use of *C. elegans* as a model for nanotoxicity, as this bacterivore worm constantly interacts with microbes in nature, which are ingested through the pharynx, the main potential route of exposure to nanoparticles is consequently oral (*Pluskota et al., 2009*). Similarly, human exposure to nanoparticles is also mostly through an oral route of entry, as nanoparticles are added to food in significant amount; the most prevalent ones being Ag, SiO_2, TiO_2 and ZnO (*Fröhlich & Roblegg, 2016*). For example, it is estimated a 70 kg individual ingests 126 mg of Ag nanoparticles per day in Europe (*Dekkers et al., 2011*). The nematode worm *C. elegans*, as a model organism, is thus valid for studying nanotoxicity in higher eukaryotic organisms such as humans. Additionally, a second route of exposure is through the worm's vulval slit, where nanoparticles interfere with vulval cells and spermatecae (*Scharf, Gührs & Von Mikecz, 2016*). However, two routes of exposure to nanoparticles that cannot be studied in C. elegans are respiratory and dermal absorption, which are prevalent routes of exposure to nanoparticles for humans (*Fröhlich & Roblegg, 2016*).

The fast phenotyping of *C. elegans* can be coupled with transcriptome profiling (i.e., gene expression microarray or RNAseq) to study underlying molecular mechanisms. For instance, using gene expression microarray, Rocheleau et al. found that *C. elegans* exposed to nano-TiO_2 showed increased expression of the glutathione S-transferase gene *gst-3* and the cytochrome P450 gene *cyp33-11*; while the oxidative stress response, as measured by the stress resistance regulator *scl-1*, showed increased expression after exposure to both nano- and bulk-sized TiO_2 (*Rocheleau et al., 2015*). In addition, the expression of *pod-2*, a reproduction-related gene, was decreased in a concentration-dependent manner with nano-TiO_2 exposure (*Rocheleau et al., 2015*). Based on the same technology, Starnes et al. identified that five lysosomal pathway related genes, including genes encoding the cysteine proteases *cpr-1* and *cpr-2*, were changed significantly after exposure to silver (Ag) nanoparticles (*Starnes et al., 2016*). To the best of our knowledge, no transcriptome profiling has been reported to investigate SiO_2 nanoparticles in *C. elegans*. The main objective of the current study is to develop and to evaluate a *C. elegans*-based animal model to study nanotoxicity by integrating comprehensive phenotyping and transcriptome profiling. We selected Ag and five metal oxide nanoparticles (SiO_2, TiO_2, CuO, Al_2O_3 and CeO_2), and measured four endpoints (locomotion velocity, growth, reproduction and

neurotoxicity) in *C. elegans* after exposure to these nanoparticles. Worms that exhibited the most significant effects were subjected to RNAseq to identify the affected biological processes and pathways. Hence, we offer a novel perspective to study nanoparticle toxicity using the soil nematode *C. elegans*.

MATERIAL AND METHODS

Caenorhabditis elegans culture

The *C. elegans* N2 strain was obtained from the Caenorhabditis Genetics Center (CGC) at the University of Minnesota. *Escherichia coli* OP50 was also obtained from the CGC and was grown for 18 h at 37 °C in Luria-Bertani (LB) broth (*Bertani, 1951*). The N2 strain was maintained at 21 °C in an incubator on Nematode Growth Media (NGM) plates and *C. elegans* were synchronized using 5.0 ml of alkaline bleach to kill the adult hermaphrodites and release their eggs (*Stiernagle, 2006*). Eggs were then washed three times with M9 buffer and left overnight on a rocking platform at room temperature to hatch into L1 larvae (*Stiernagle, 2006*).

Preparation of nanoparticles

Ag, SiO_2, CuO, Al_2O_3, and CeO_2 nanoparticles were purchased from Sigma-Aldrich (St. Louis, USA). TiO_2 nanoparticles were obtained from the Joint Research Center of (JRC) the European Commission. All nanoparticles were less than 100 nm in size as described by the manufacturer and commission. Product details are shown in Table 1. Nanoparticles were dissolved at stock concentration of 1,000 μg/ml in ddH_2O and sonicated using an Ultrasonic Processor VCX (GEX) 750 at an amplitude of 40% for a 3-minute pulse, followed by 1 min on ice. This step was repeated five times to ensure complete disaggregation of the nanoparticles. Nanoparticle solutions were then diluted to working concentrations of 200 μg/ml in S-medium (*Jung et al., 2015*).

Locomotion velocity and growth (body length) assays

200 L1 stage *C. elegans* N2, obtained after synchronization with alkaline bleach, were grown in S-medium in 6-well plates containing 0 (control), 10 or 50 μg/ml of each nanoparticle, supplemented with *E. coli* OP50 at a final optical density at 595 nm (OD_{595}) of 1, for 72 h at 21 °C until they reached the day 1 adult stage. For the locomotion velocity endpoint assay, worms were then washed once in 1X M9 buffer and placed on unseeded NGM plates and allowed to explore their surroundings for 10 min. Worms ($n = 14$ to 111 per condition) were then recorded using a Nikon camera (SMZ1270) linked to a computer. The average locomotion velocity of each worm was calculated for 30 s at an interval of 0.500 ms using the software (NIS-Elements, version 4.60) accompanying the camera. The average locomotion velocity was calculated by averaging the locomotion velocity (in μm/s) over the 30 s of recording. For the growth (body length) endpoint assay, worms were grown in the same manner as in the locomotion velocity endpoint assay, washed once in 1X M9 buffer and killed with 10 mM sodium azide. Dead worms were transferred to an unseeded NGM plate to take pictures. The body length of worms ($n = 20$ to 43 per condition), measured in μm, was calculated using the camera's software (NIS-Elements, version 4.60).

Table 1 Product details of six different nanoparticles. Each nanoparticle, used in this study, is smaller than 100 nm in size. NA: non-applicable (no information provided from the suppliers).

Nanoparticle	Symbol	Catalog number/Brand	CAS number	Size (nm)	Shape
Silver	Ag	576832/Aldrich	7440-22-4	<100	Spherical
Silicon dioxide	SiO_2	637238/Aldrich	7631-86-9	10-20 (BET)	Spherical
Cerium(IV) oxide	CeO_2	544841/Aldrich	1306-38-3	<25 (BET)	NA
Copper(II) oxide	CuO	544868/Aldrich	1317-38-0	<50 (TEM)	NA
Aluminum oxide	Al_2O_3	544833/Aldrich	1344-28-1	<50 (TEM)	NA
Titanium dioxide	TiO_2	NM-101/JRC	NA	8	NA

Reproduction (brood size) assay

200 L1 *C. elegans* N2, obtained by synchronization, were grown for 48 h at 21 °C to the L4-young adult stage on *E. coli* OP50-seeded NGM plates. Five L4-young adult hermaphrodites were transferred to an individual well in quadruplicate of a 12-well plate containing S-medium supplemented with either 0 (control), 10 or 50 µg/ml of each nanoparticle and *E. coli* OP50. The L4-young-adult hermaphrodites were then allowed to grow and lay eggs for 96 h, and resulting progeny were counted by dilution.

Neurotoxicity (number of head thrashes) assay

200 L1 *C. elegans* N2 were grown to the adult day 1 stage (72 h at 21 °C) in individual wells of a 6-well plate containing S-medium containing either 0 (control), 10 or 50 µg/ml of each nanoparticle and *E. coli* OP50. A total of 1.0 ml of the well contents were centrifuged at 1,000 rpm for 2 min, the supernatant was decanted, leaving the worm pellet undisturbed. Worms were then washed in 1X M9 buffer and centrifuged at 1,000 rpm for 2 min. Worms were then transferred to an unseeded NGM plate containing 60 µl of K-medium (2.36 g of KCl and 3.0 g NaCl per liter of media dissolved in ddH_2O). Individual adult day 1 stage *C. elegans* were transferred into the drop of K-medium. Worms were allowed to swim freely for 1 min. Afterwards, the number of head thrashes of each individual worm ($n = 8$ to 55 per condition) were counted for 1 min as described by *Tsalik & Hobert (2003)*.

Total RNA extraction of worms exposed to Ag and SiO_2 nanoparticles

400 L1 *C. elegans* N2 were grown in individual wells of a 12-well plate containing either 0, 10 µg/ml Ag nanoparticles or 10 µg/ml SiO_2 nanoparticles and supplemented with *E. coli* OP50, until the worms reached the adult day 1 stage (72 h at 21 °C). Each condition was repeated six times. The contents of the wells were centrifuged at 1,000 rpm for 2 min, the supernatant was decanted and the worm pellet was washed twice with 1X M9 buffer. 200 µl of Trizol (Ambion, USA) was then added to the worm pellet. The worm pellet then was flash-frozen in liquid nitrogen, followed by a quick thaw. These two steps were repeated once. RNA from the resulting worm pellet-Trizol solution was extracted using the Direct-zol RNA miniprep kit (Zymo Research, USA) according to the manufacturer's instructions. Quantity and purity of total RNA were checked using a spectrophotometer (ND-1000, NanoDrop). The RNA samples were then sent to the McGill University and Génome Québec Innovation Centre (http://gqinnovationcenter.com) for quality analysis

with Bioanalyser and for single-end read (100 base) RNA sequencing under HiSeq 2500 (Illumina).

Data analysis for RNAseq

Raw data for each sample was received in fastq file format from the McGill University and Génome Québec Innovation Centre. Read quality was checked with FASTQC (version 0.11.3) and adapter related sequences were removed using Trim Galore (version 0.4.5) (https://www.bioinformatics.babraham.ac.uk/projects/). The genome sequence of *C. elegans* and GTF file (Caenorhabditis_elegans.WBcel235.91.gtf) were downloaded from ENSEMBL (https://www.ensembl.org/). Reads were aligned to the *C. elegans* genome with HISAT2 (version 2.1.0) (*Kim, Langmead & Salzberg, 2015*) and sorted alignment files were generated by SAMtools (version 1.7) (*Li et al., 2009*). Raw read counts were extracted using HTSeq (version 0.9.1) with the intersection-strict mode (*Anders, Pyl & Huber, 2015*). Entrez IDs were extracted from a Bioconductor package (org.Ce.eg.db) (*Carlson, 2018*) and assigned to the wormbase gene sequences using R. Sample distribution by principal component analysis was visualised using NetworkAnalyst 3.0 (*Zhou et al., 2019*). Differential gene expression analysis between the nanoparticle treatments and control was carried out using edgeR where data were normalised by trimmed mean of M-values (TMM) and tag-wise dispersion parameters were estimated using the empirical Bayes method (*Robinson, McCarthy & Smyth, 2010*). For gene set enrichment analysis, genes were ranked by the expression ratio (combination of log2 fold change and FDR) and normalized enrichment score (NES) was determined using GSEAPreranked in Gene Set Enrichment Analysis (GSEA; version 3.0) (*Subramanian et al., 2005*). The value for the parameter of min size: exclude smaller sets was set to 0, the value for permutations was set to 1000 and the enrichment statistic was set to classic. For use with GSEAPreranked, GO derived MSigDB format gene sets for *C. elegans* was downloaded from GO2MSIG (*Powell, 2014*) and KEGG database of *C. elegans* was extracted from a current Bioconductor package (version 3.7) (*Luo et al., 2009*) and converted to *gmt file. Pathway interaction was investigated using ClueGO (*Bindea et al., 2009*). Furthermore, gene enrichment in GO and newly determined terms were carried out using GOATOOLS (*Klopfenstein et al., 2018*) and WormExp (*Yang, Dierking & Schulenburg, 2016*), respectively. Differentially expressed genes in the toxicity groups (compared to control) were further searched to ascertain whether they were reported in metal toxicity based on previous studies (*Caito et al., 2012*; *Cui et al., 2007*; *Roh, Lee & Choi, 2006*; *Kumar et al., 2015*; *Anbalagan et al., 2012*).

Statistical analysis

Statistical analysis was performed using GraphPad Prism (version 8.0.0). The statistical difference between the groups in the toxicity assays was evaluated with One-way ANOVA followed by Dunnett's multiple comparison test and P value less than 0.05 was accepted as statistically significant.

RESULTS

The pooled average locomotion velocity for *C. elegans* grown under control conditions was 150.1 μm/s across all treatments, indicating that worms are active after growth

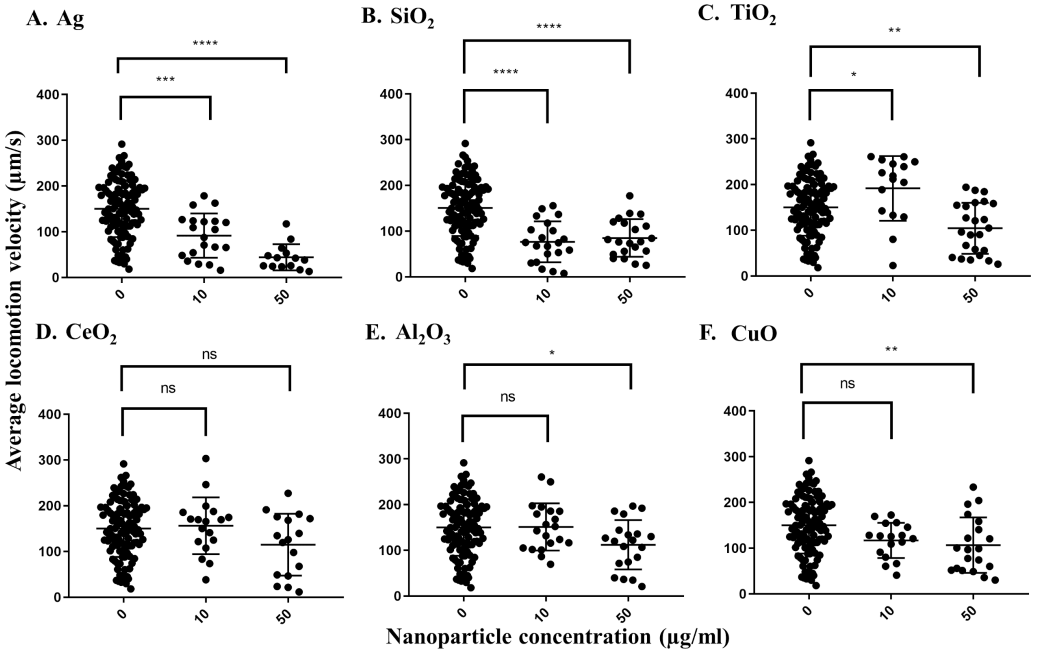

Figure 1 Average locomotion velocity of adult day 1 *C. elegans* N2 after exposure to various nanoparticles (A, Ag; B, SiO_2; C, TiO_2; D, CeO_2; E, Al_2O_3; and F, CuO) at 0, 10 and 50 µg/ml. A total of 200 L1s were grown in 6-well plates containing S-medium supplemented with described concentrations of each nanoparticle for 72 h at 21 °C. After washing and transferring the worms onto an unseeded NGM plate, adult day 1 *C. elegans* were then video-recorded for 30 s using a Nikon camera and average locomotion velocity was calculated using corresponding software for every 0.500 msec over the 30 s time span. Only Ag and SiO2 nanoparticles show significant reductions in the velocity parameter at 10 µg/ml in comparison with control ($P < 0.0001$). Each point represents a single worm. Statistical difference is indicated with an asterisk (*) (*$P < 0.05$, ** $P < 0.01$, *** $P = 0.0001$, **** $P < 0.0001$ and ns: non-significant).

Full-size DOI: 10.7717/peerj.8684/fig-1

in S-medium for 72 h at 21 °C. In comparison, the average locomotion velocity of worms decreased to 91.5 µm/s in the presence of 10 µg/ml Ag nanoparticles and further reduced to 44.2 µm/s in the presence of 50 µg/ml Ag nanoparticles, which was statistically significant for each concentration ($P = 0.0001$ and $P < 0.0001$, respectively) (Fig. 1A). Additionally, the difference in the reduction levels by the concentrations (>50%) indicated a dose-dependent decrease in average locomotion velocity in response to increasing Ag nanoparticle concentration. The second nanoparticle to influence the worms' average locomotion velocity was SiO_2, which caused significant decreases at 10 or 50 µg/ml doses in comparison with control ($P < 0.0001$ for both concentrations). Surprisingly, it appeared that TiO_2 nanoparticles increased *C. elegans* average locomotion velocity at 10 µg/ml ($P = 0.0257$), although this could be a statistical artifact due to sampling effect based on the data distribution (Fig. 1C). Al_2O_3-, TiO_2- and CuO-treated *C. elegans* showed decreases in average locomotion velocity when tested at 50 µg/ml ($P = 0.0196$, for Al_2O_3 and $P < 0.005$ for both TiO_2 and CuO), displaying locomotion velocities of 104.4, 114.8 and 112.2 µm/s, respectively (Figs. 1C–1E). CeO_2 nanoparticles had no effect at any of the concentrations tested ($P > 0.05$, for both concentrations).

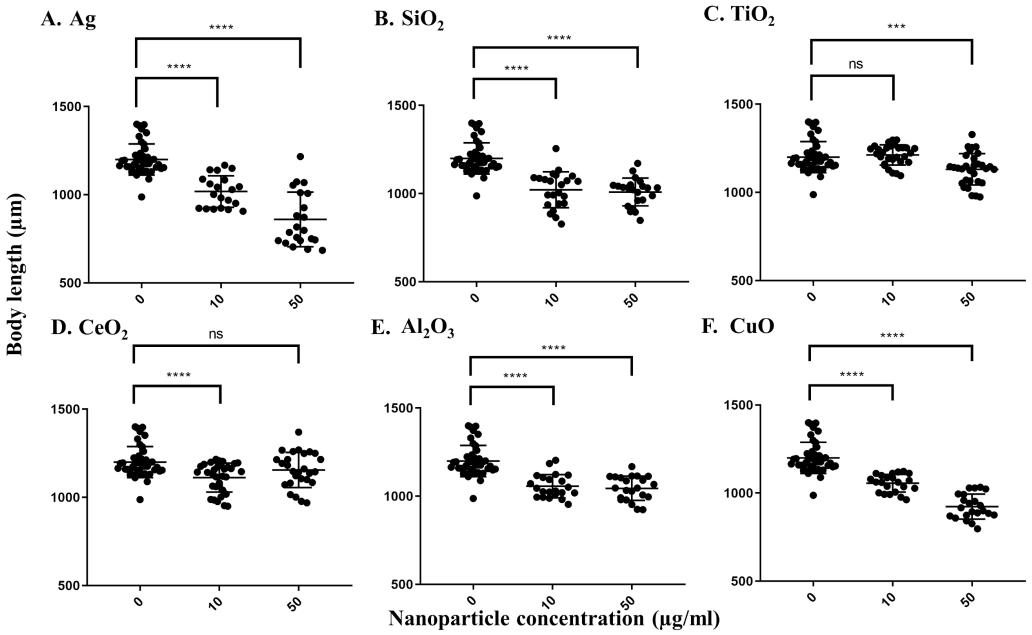

Figure 2 Body length of adult day 1 *C. elegans*. N2 after exposure to various nanoparticles (A, Ag; B, SiO_2; C, TiO_2; D, CeO_2; E, Al_2O_3; and F, CuO) at 0, 10 and 50 µg/ml. 200 L1s were grown in 6-well plates containing S-medium supplemented with described concentrations of each nanoparticle for 72 h at 21 °C. Worms were killed using 10 mM sodium azide and transferred onto an unseeded NGM plate. Worms were photographed using a Nikon camera and body length was determined using corresponding software. All the nanoparticles except TiO_2 demonstrated reductions in the body length at 10 µg/ml, compared to control ($P < 0.0001$). Each point represents a single worm.

Full-size DOI: 10.7717/peerj.8684/fig-2

For the growth inhibition (body length) assay, Ag nanoparticles had the greatest effect. The pooled average body length of worms grown in the control S-medium after a three-day incubation at 21 °C was 1199.6 µm, indicating that the worms grew efficiently in this medium. As with the locomotion velocity endpoint assay, a concentration-dependent decrease in body length was observed when worms were exposed to different concentrations of Ag nanoparticles, with average body lengths of 1017.8 µm under 10 µg/ml and 859.3 µm under 50 µg/ml, respectively ($P < 0.0001$ for both concentrations) (Fig. 2A). Exposure to SiO_2 nanoparticles induced significant decrease at 10 µg/ml ($P < 0.0001$) (Fig. 2B), but no further significant decrease was observed at 50 µg/ml. Exposure to CuO nanoparticles also resulted in a concentration-dependent decrease in body length, leading to an average body length of 1055.3 and 923.1 µm, respectively ($P < 0.0001$ for both concentrations) (Fig. 2F). For CeO_2 and Al_2O_3 nanoparticles, significant decreases in body length were observed at 10 µg/ml compared to control worms ($P < 0.0001$, Figs. 2D and 2E). For TiO_2 nanoparticles, a significant difference was observed only at 50 µg/ml, in which the exposed worms showed an average body length of 1130.8 µm ($P = 0.001$) (Fig. 2C). In summary, these results show Ag and SiO_2 nanoparticles have similar toxicity on *C. elegans*, although the effect appears to be concentration-dependent for Ag nanoparticles whereas there is likely a threshold effect for SiO_2 nanoparticles.

To measure the effects of the various nanoparticles on *C. elegans* reproduction, we incubated five L4-young adults in S-medium supplemented with *E. coli* OP50 and the respective nanoparticles for four days (96 h) at 21 °C. It was expected that each worm would lay approximately 300 eggs in that time span, so that the total number of progeny per 5 worms would be near 1,500 under control conditions (*Sulston & Hodgkin, 1988*; *Sonowal et al., 2017*). The average control value of progeny produced by 5 worms under our experimental conditions was 1,288 after 96 h. We found that most nanoparticles reduced the number of progeny produced by *C. elegans*. At 10 μg/ml, Ag nanoparticles decreased the brood size of *C. elegans* to around 37%, which was statistically significant ($P < 0.0001$) (Fig. 3A). The effect was even more pronounced at 50 μg/ml, as Ag nanoparticles decreased the number of progeny to 33% of the control value, suggesting that these nanoparticles do indeed decrease *C. elegans* brood size ($P < 0.0001$) (Fig. 3A). On the other hand, SiO_2 nanoparticles decreased brood size substantially at both 10 μg/ml and 50 μg/ml ($P < 0.0001$) (Fig. 3B), indicating that SiO_2 nanoparticles are potent inhibitors of *C. elegans* reproduction in concentrations ranging in μg/ml. In contrast, TiO_2 nanoparticles, known to inhibit *C. elegans* reproduction, reduced brood size to about 80% of the control value in our testing concentration range (Fig. 3C). CeO_2 nanoparticles inhibited *C. elegans* reproduction as well. The brood size decreased to 55% of the control-treated value at a concentration of 10 μg/ml ($P = 0.0002$) (Fig. 3D). Interestingly, at 50 μg/ml, the decrease was not as pronounced, equating to 89% of the control-treated value ($P > 0.05$) (Fig. 3D). This observation may be due to the aggregation of CeO_2 at higher concentrations. Al_2O_3 nanoparticles did not show statistically significant effects on *C. elegans* under our conditions ($P > 0.05$) (Fig. 3E), whereas CuO nanoparticles decreased the brood size value to 83% and 71% of the control value, at 10 μg/ml and 50 μg/ml, respectively (Fig. 3F).

Both Ag and SiO_2 nanoparticles showed no significant impact of the number of head thrashes based on a population of worms in 60 s at 10 μg/ml versus control worms (Figs. 4A and 4B). SiO_2 nanoparticles showed a slight effect on the neurotoxicity assay at 50 μg/ml ($P = 0.0033$), whereas Ag nanoparticles had no such effect on neurotoxicity. Similar results were observed for TiO_2 and nanoparticles at both concentrations tested (Fig. 4C). In contrast, CeO_2, Al_2O_3 and CuO nanoparticles showed significant effects on neurotoxicity at 10 μg/ml under our conditions, as determined by a significant decrease in the number of head thrashes, and this trend was conserved at 50 μg/ml ($P < 0.0001$ for both CeO_2concentrations, $P = 0.0087$ and $P < 0.0001$ for Al_2O_3 at 10 μg/ml and 50 μg/ml, respectively and $P = 0.0002$ for CuO at 10 μg/ml), although the effect on neurotoxicity of CuO nanoparticles at 50 μg/ml was not significant ($P > 0.05$) (Figs. 4D and 4F).

Based on the phenotyping results, we further performed RNAseq analysis on *C. elegans* exposed to Ag and SiO_2(10 μg/ml) as these two nanoparticles demonstrated the most outstanding effect on majority of the parameters (locomotion velocity, growth and reproduction). For each sample (5 replicates for the Ag, SiO2 and control groups), around 20 million reads were obtained. Approximately 97% of reads were mapped to the worm's genome and a total of 18,861 gene sequences were identified, using a minimal total read count of 3 across samples. Sample distribution by principal component analysis (PCA) is shown in Fig. S1. Differentially expressed genes (DEGs) based on edgeR between control

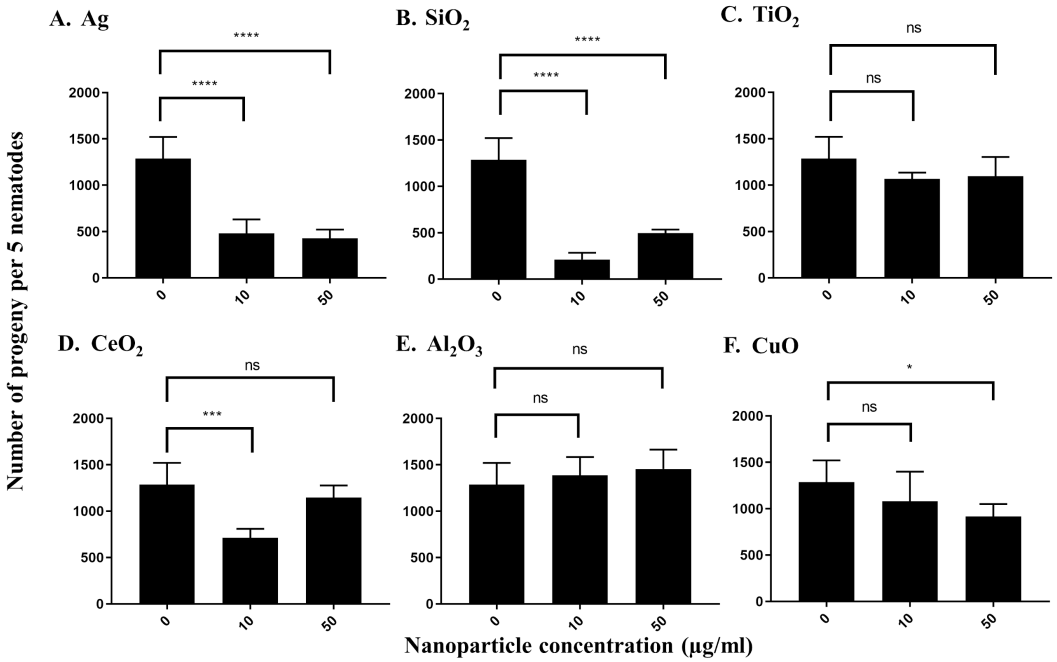

Figure 3 Reproduction capacity of *C. elegans* N2 after exposure to various nanoparticles (A, Ag; B, SiO_2; C, TiO_2; D, CeO_2; E, Al_2O_3; and F, CuO) at 0, 10 and 50 µg/ml. 200 L1s obtained from synchronization were seeded onto *E. coli* OP50-coated NGM plates and grown to the L4-young adult stage (48 h at 21 °C). Five L4-young adults were then transferred to a single well of a 12-well plate containing S-medium with corresponding concentrations of nanoparticles (0,10 and 50 µg/ml). Plates were then incubated for 96 h at 21 °C. The resulting total number of progeny was then calculated by dilution. Ag, SiO_2 and CeO_2 nanoparticles reduced the reproduction capacity in comparison with control significantly at 10 µg/ml ($P < 0.0001$). Bar-graphs represent average brood size ± standard deviation (SD) per five L4-young adult nematodes per condition.

Full-size DOI: 10.7717/peerj.8684/fig-3

and the toxicity groups (2,648 DEGs in the Ag group and 1,087 DEGs in the SiO2 group) are shown in Data S1 (FDR < 0.05).

Gene set enrichment analysis (GSEA) based on Gene Ontology biological processes (BPs) showed various statistically enriched positively or negatively based on the fold changes and running enrichment scores (Data S2). The top 20 and phenotype reflecting enriched BPs are shown in Table 2 (FDR < 0.05). These BPs were related to various physiological events such as cellular and metabolic responses. *Apoptotic process* showed gene enrichment with positive NES in both Ag and SiO2 groups under significant levels (FDR < 0.0001). Phenotype reflecting BPs including regulation of locomotion, reproductive process and cell growth were enriched with negative NES significantly (FDR < 0.0001 for regulation of locomotion, FDR = 0.001 for regulation of reproductive process, FDR = 0.002 for regulation of cell growth in the Ag group; FDR < 0.0001 for regulation of locomotion, FDR = 0.008 for regulation of reproductive process, FDR = 0.042 for regulation of cell growth in the SiO2 group) (Fig. 5). A number of genes were commonly detected within the top five category in the phenotype reflecting enriched BPs for both Ag and SiO2 groups, including transcription factor (che-1) and MiRP K channel accessory subunit (mps-1) in

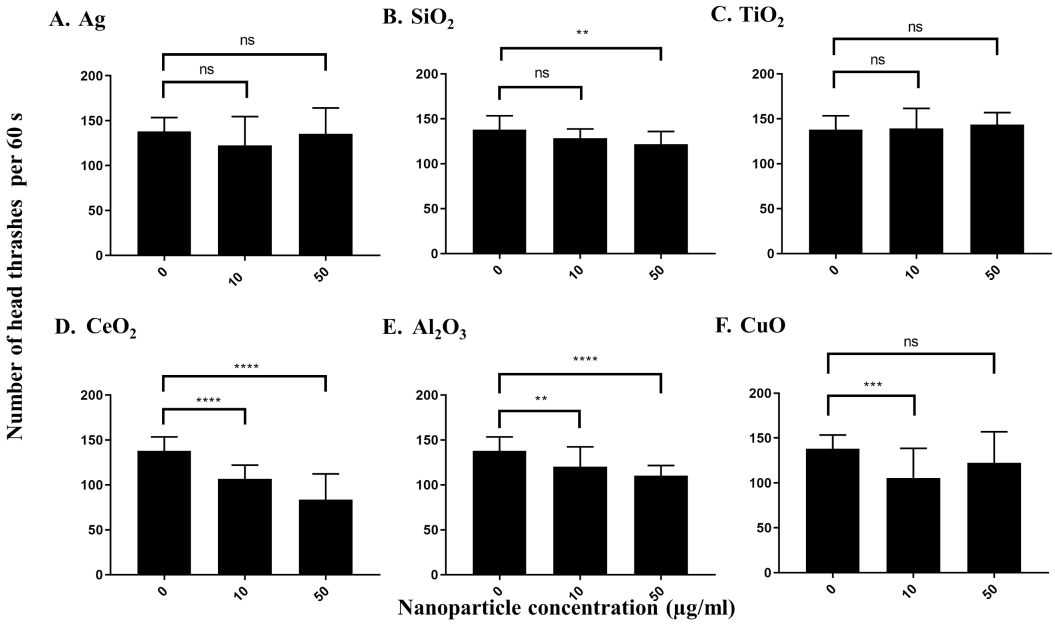

Figure 4 Neurotoxicity of various nanoparticles (A, Ag; B, SiO_2; C, TiO_2; D, CeO_2; E, Al_2O_3; and F, CuO) to *C. elegans* N2 at 0, 10 and 50 µg/ml. 200 L1s were grown in 6-well plates containing S-medium supplemented with described concentrations of each nanoparticle for 72 h at 21 °C. Adult day 1 worms were then washed and put into an unseeded NGM plate containing K-medium and allowed to swim freely for 60 s. The number of head thrashes made by a single worm were then counted for 1 minute. Only three nanoparticles, CeO_2, Al_2O_3 and CuO, show significant differences for the neurotoxicity parameter at 10 µg/ml, compared to control ($P < 0.01$). Bar-graphs represent average number of head thrashes ±SD per condition.

Full-size DOI: 10.7717/peerj.8684/fig-4

regulation of locomotion, caveolin (cav-1) in regulation of reproductive process, and cyclic nucleotide-gated cation channel (tax-4) and protein let-756 (let-756) in regulation of cell growth (Data S2).

The other significantly enriched BPs were associated with various physiological events and immune defense of the organism. As both Ag and SiO_2 nanoparticles were foreign substances for the worm, we further examined the expression profiles of genes associated with innate immunity. Compared to Ag and Control, SiO_2 exposure led to significant downregulations of genes related to the innate immune response (FDR < 0.0001) (Fig. 6).

The enriched BPs by GOATOOLS were mainly related to the physiological events, of which, some were identical to those observed by the GSEA analysis (Data S2). However, the number of the BPs detected by GOATOOLS was lower compared to those detected by GSEA, which was likely related to the differences in gene inputs (DEGs with FDR < 0.05 vs cut-off free DEGs ranked by fold change) and/or the methodologies used. Nevertheless, the phenotype reflecting BPs including the regulations of locomotion and reproductive process were also enriched in the Ag group in the GOAtools analysis. However, this was not the case for the SiO2 group, which appeared to be related to lower number of DEGs in this group, compared to the Ag group.

Table 2 Top 20 and phenotype reflecting enriched biological processes. The enriched biological processes, ranked based on NES and FDR value, are shown. The enriched biological processes, detected by the GSEA analysis, were statistically significant (no asterisk: FDR < 0.0001, *: FDR < 0.05 and **: FDR < 0.01). The phenotype reflecting enriched biological processes are shown under dashed-line ‡: Full name is provided in Data S2.

		Ag			SiO2		
	Biological process		**NES**	**Rank**		**NES**	**Rank**
Positive enrichment							
	Cellular process	Cell cycle	6.591	2	Cell cycle	4.095	2
		Cell cycle process	6.624	1	Cell cycle process	4.167	1
		Meiotic cell cycle	5.455	10	Meiotic cell cycle	3.413	10
		Meiotic cell cycle process	4.744	15	_	_	_
		Meiotic nuclear division	5.215	12	Meiotic nuclear division	3.158	12
		Meiotic chromosome segregation	4.441	18	_	_	_
		Mitotic cell cycle	4.805	14	Mitotic cell cycle	2.776	19
		Regulation of cell cycle	4.378	20	_	_	_
		Cell division	4.561	17	Cell division	2.886	14
		Death&cell death	6.022	4	Death&cell death	3.699	7
		Programmed cell death	5.736	7	Programmed cell death	3.695	8
		Apoptotic process	6.332	3	Apoptotic process	3.887	5
		Chromosome segregation	4.943	13	_	_	_
		Posttranscriptional gene silencing&gene silencing	4.407	19	_	_	_
	Growth	_	_	_	Developmental growth	2.771	20
		_	_	_	Regulation of growth	2.787	18
	Metabolic process	Posttranscriptional regulation of gene gene expression	4.571	16	_	_	_
	Multicellular organism process	_	_	_	Positive regulation of multicellular organismal process	2.814	16
	Multi-organism process	Sexual reproduction	5.713	8	Sexual reproduction	3.854	6
		Gamete generation	5.982	5	Gamete generation	4.012	3
		Germ cell development&cellular process †	5.334	11	Germ cell development& cellular process †	3.897	4
		_	_	_	Female gamete generation	2.813	17
		_	_	_	Oogenesis	3.010	13
		_	_	_	Spermatid differentiation& spermatid development	2.818	15
	Cellular component organization or biogenesis	Organelle fission	5.756	6	Organelle fission	3.433	9
		Nuclear division	5.621	9	Nuclear division	3.364	11

(*continued on next page*)

Table 2 (*continued*)

	Biological process	Ag	NES	Rank	SiO2	NES	Rank
Negative enrichment							
	Behavior	Single organism behavior	−4.631	1	_	_	_
	Cellular process	Cell communication	−4.285	7	Aromatic compound biosynthetic process	−5.477	11
		Cell surface receptor signaling pathway	−4.082	17	Regulation of cellular metabolic process	−5.198	19
	Developmental process	Cell morphogenesis	−4.571	3	_	_	_
		Cell projection morphogenesis	−4.576	2	_	_	_
		Cell part morphogenesis	−4.276	8	_	_	_
		Generation of neurons	−4.048	20	_	_	_
	Metabolic process						
		_	_	_	Cellular nitrogen compound biosynthetic process	−5.306	16
		_	_	_	Heterocycle biosynthetic process	−5.423	12
		_	_	_	Nucleobase containing compound biosynthetic process	−5.486	10
		_	_	_	Organic cyclic compound biosynthetic process	−5.323	15
		_	_	_	Positive regulation of gene expression	−5.029	20
		_	_	_	Regulation of biosynthetic process& †	−5.410	13
		_	_	_	Regulation of macromolecule biosynthetic process	−5.267	17
		_	_	_	Regulation of cellular macromolecule biosynthetic process	−5.260	18
		_	_	_	Regulation of nitrogen compound metabolic process& †	−5.587	9

(*continued on next page*)

Table 2 (*continued*)

	Biological process	Ag	NES	Rank	SiO2	NES	Rank
		–	–	–	Regulation of primary metabolic process	−5.406	14
		Regulation of rna metabolic process	−4.138	15	Regulation of rna metabolic process	−5.971	2
		Rna biosynthetic process	−4.198	12	Rna biosynthetic process	−5.923	3
		Nucleic acid templated transcription	−4.121	16	Nucleic acid templated transcription	−5.833	6
		Regulation of rna biosynthetic process	−4.164	14	Regulation of rna biosynthetic process	−5.983	1
		Transcription dna templated	−4.200	11	Transcription dna templated	−5.864	5
		Regulation of transcription dna templated& †	−4.062	19	Regulation of transcription dna templated& †	−5.805	7
		Transcription from rna polymerase ii promoter	−4.268	9	Transcription from rna polymerase ii promoter	−5.881	4
		Regulation of transcription from rna poly. †	−4.192	13	Regulation of transcription from rna poly. †	−5.775	8
	Multicellular organism development	Nervous system development	−4.528	4	–	–	–
	Response to stimulus	Response to external stimulus	−4.493	5	–	–	–
		Taxis	−4.066	18	–	–	–
	Signaling	Signaling	−4.266	10	–	–	–
		Single organism signaling	−4.299	6	–	–	–
Phenotype reflecting							
	Growth	Regulation of cell growth**	−2.326	167	Regulation of cell growth*	−1.714	410
	Locomotion	Regulation of locomotion	−3.124	66	Regulation of locomotion	−3.694	86
	Reproduction	Regulation of reproductive process**	−2.476	132	Regulation of reproductive process**	−2.062	294

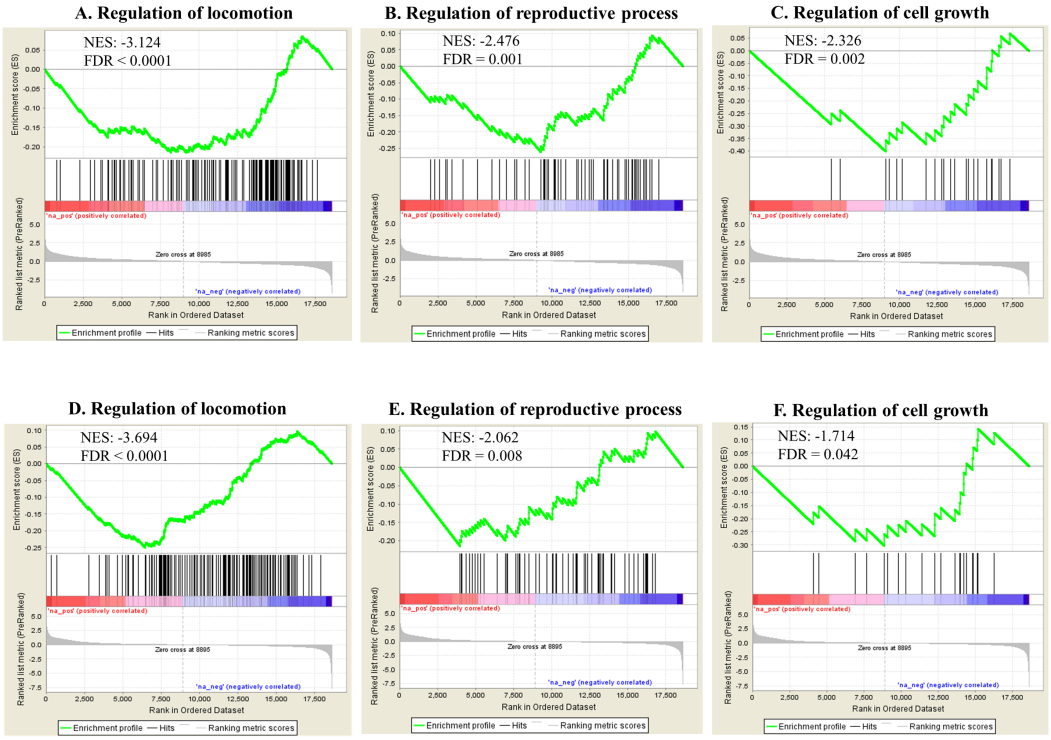

Figure 5 Selected significant GO terms (detected by GSEA). Enriched BPs including regulation of locomotion, regulation of reproductive process and regulation of cell growth, show negative NES in the Ag group (A–C) and the SiO2 group (D–F) (FDR < 0.05).

Full-size DOI: 10.7717/peerj.8684/fig-5

Analysis of the RNAseq data using WormExp showed gene enrichment in newly determined terms (Data S2). Some of these terms were found associated with regulations of locomotion, reproduction and cell growth in both groups. The "glp-1 mutant" term was enriched in the Ag and SiO2 groups, which refers to the diminished reproductive capability of *C. elegans* (*Gracida & Eckmann, 2013*). In regard to development terms, "pgl-1 mutant" and "P-granule RNAi" were enriched in the Ag and SiO2 groups, respectively, linking regulation of cell growth (*Knutson et al., 2017*). The "wdr-23 mutant" term was also present for both nanoparticle exposure groups. This is notable as wdr-23, through the action of skn-1, is involved in proper locomotion of *C. elegans* (*Staab et al., 2013*). Finally, the other terms, including regulation by heavy metals/NPs (such as Ag), were found for both groups, further validating the nanoparticle effect. Altogether, the WormExp gene enrichment terms, obtained from the RNAseq data, appear to be in agreement with the phenotypic assay results.

Pathway enrichment analysis against the KEGG database showed various significantly enriched pathways (Data S3). The top 20 enriched biological pathways are shown for both exposures in Table 3. Ribosome, proteasome, aminoacyl-tRNA biosynthesis and RNA transport were significantly upregulated in both groups, indicating overall higher rate of protein turnover upon exposure. In contrast, biological pathways reflecting phenotypes including neuroactive ligand–receptor interaction [regulating locomotion

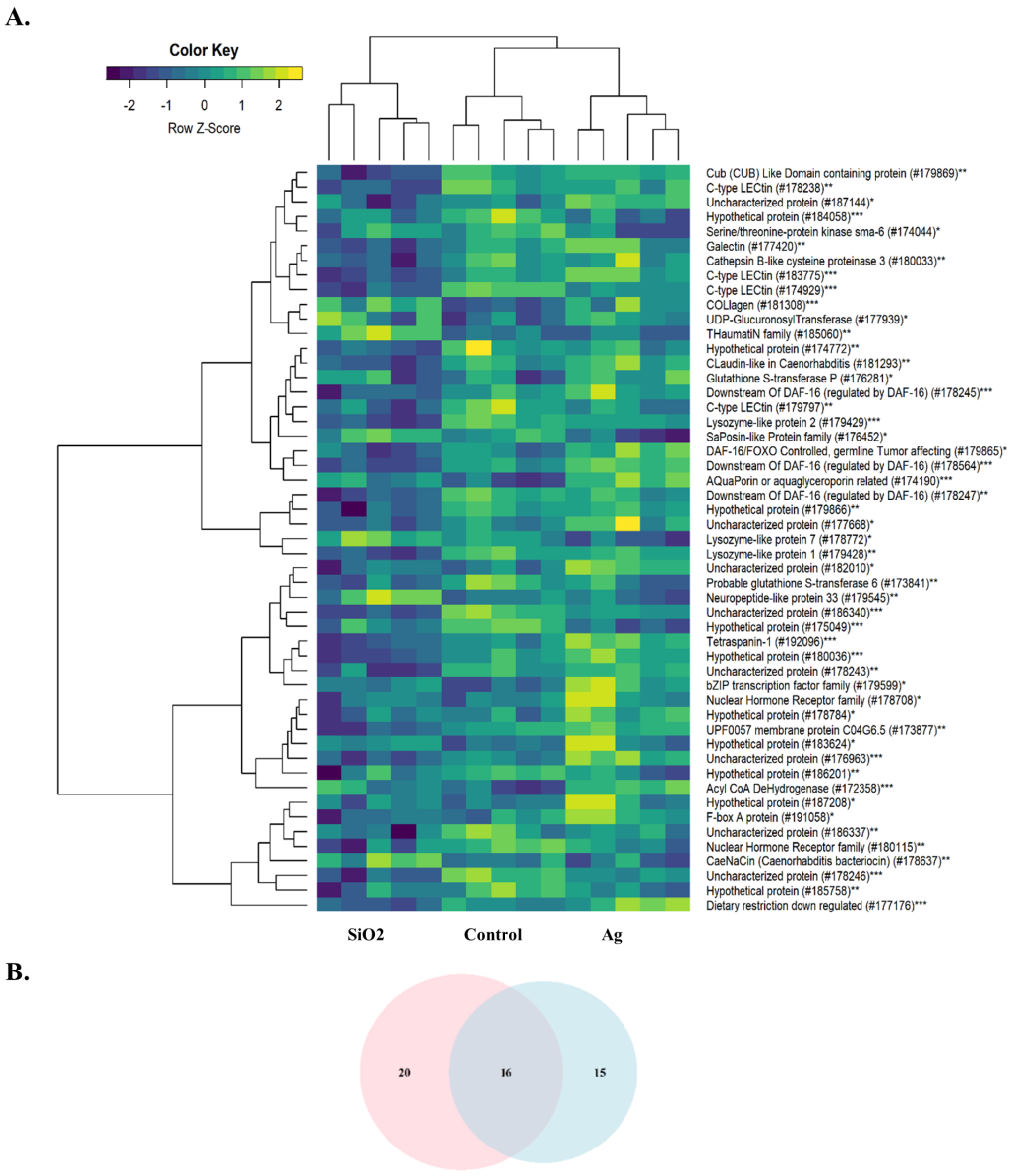

Figure 6 Heatmap of differentially expressed genes involved in the innate immune response. A down-regulation pattern is observed in the SiO_2 group, in comparison with the Ag group and Control (A). Pink and blue circles in Venn diagram represents differentially expressed genes in the SiO2 and Ag groups, respectively (B). *: Ag, **: SiO2, ***: Common for Ag and SiO2.

Full-size DOI: 10.7717/peerj.8684/fig-6

(*Kong et al., 2015*)], wnt-signaling (regulating reproduction and cell growth (*Inoki et al., 2006*; *Hernandez Gifford, 2015*) and MAPK signaling (regulating reproduction and cell growth (*Zhang & Liu, 2002*; *Andrade et al., 2014*) were significantly down-regulated in both exposures (Fig. 7). Some genes were found commonly within the top 5 enriched gene category in each enriched biological pathway for both Ag and SiO_2 treatments (based on fold change and running enrichment score), which were tachykinin receptor family (tkr-2),

serotonin/octopamine receptor family (ser-1) in neuroactive ligand–receptor interaction pathway, skp1 related (ubiquitin ligase complex component, skr-8, skr-10, skr-12) in wnt signaling pathway, protein ver-1 (ver-1) and heat shock protein (hsp 70) in MAPK signaling pathway (Data S3).

DISCUSSION

As the use of nanoparticles has increased dramatically in recent years, there is a growing concern regarding their potential impact to environment and human health. In this study, we have systematically evaluated a *C. elegans*-based animal model for nanotoxicity assessment. Our results have shown that Ag and SiO_2 have the most potent toxic effect on locomotion velocity and growth, as well as reproduction (brood size), but not on neurotoxicity. In this model, the transcriptome profile is concordant with the phenotype characteristic for both exposures (Fig. 8).

The top 20 GO BPs identified by the GSEA were related to various physiological events in the Ag and SiO2 toxicities. The exposure to both nanoparticles downregulated multiple regulatory biological processes, including regulation of locomotion, regulation of reproduction and regulation of cell growth, which was consistent with the phenotype profiling of our study.

Dysfunction of the enriched genes including transcription factor che-1 (che-1) and MiRP K channel accessory subunit (mps-1) (regulation of locomotion), caveolin (cav-1) (regulation of reproductive process), and cyclic nucleotide-gated cation channel (tax-4) and protein let-756 (let-756) (regulation of cell growth), have been previously shown to hinder the worm's biological events (*Uchida et al., 2003*; *Bianchi et al., 2003*; *Scheel et al., 1999*; *Komatsu et al., 1996*; *Roubin et al., 1999*). Inactivation of che-1 (mediating chemotaxis through ASE neurons) and of mps-1 (a voltage-gated pore-forming potassium subunit) impairs neuronal activities such as chemotaxis and locomotion (*Uchida et al., 2003*; *Bianchi et al., 2003*). Caveolin-1 (cav-1), identified in the adult germ line and highly expressed in eggs, is required for Ras/MAP-kinase-dependent progression (*Scheel et al., 1999*). Inhibition of tax-4 and let-756 genes hinders chemosensation and results in larval arrest, respectively (*Komatsu et al., 1996*; *Roubin et al., 1999*).

Although biological processes reflecting phenotypes were similar between both toxicities in our study, SiO_2 nanoparticles induced a remarkable downregulation pattern in innate immune response, compared to Ag and Control. In particular, several C-type lectins, which are known to be important components in innate immunity (*Mayer, Raulf & Lepenies, 2017*), appeared to be exclusively downregulated by SiO_2 nanoparticles. The subject of nanoparticle exposure and the effects on immune system has been an active research area (*Boraschi et al., 2017*). Exposure to nanoparticles has been linked to changes in the immune response such as inflammation, hypersensitivity and immunosuppression and has been shown to induce such responses through antigen-presenting cells in humans, highlighting the interaction between nanoparticles and the innate immune response (*Alsaleh & Brown, 2018*). Biocoronas, formed by the interaction of the nanoparticle surface with proteins and lipids, are highly reactive immunologically and have recently gained the attention of regulatory agencies (*Shannahan, 2017*).

Table 3 Top 20 enriched biological pathways. Ranking of the enriched biological pathways is based on NES and FDR value. The enriched biological pathways (KEGG) by the enrichment analysis were found under statistically significant levels (FDR < 0.05) except those indicated with asterisk (*: 0.05 < P < 0.13; 0.12 < FDR < 0.21).

	Ag			SiO2		
	Biological pathway	**NES**	**Rank**	**Biological pathway**	**NES**	**Rank**
Positive enrichment	Ribosome	7.179	1	Ribosome	6.864	1
	Proteasome	4.731	2	Proteasome	3.682	2
	Rna transport	4.484	3	Aminoacyl-trna biosynthesis	3.296	3
	Spliceosome	4.453	4	Oxidative phosphorylation	2.986	4
	Oxidative phosphorylation	4.320	5	Carbon metabolism	2.969	5
	Aminoacyl-trna biosynthesis	4.078	6	Rna transport	2.955	6
	Ribosome biogenesis in eukaryotes	3.661	7	Pyruvate metabolism	2.724	7
	Nucleotide excision repair	3.643	8	Rna polymerase	2.439	8
	Carbon metabolism	3.458	9	Fanconi anemia pathway	2.337	9
	Glycosylphosphatidylinositol (gpi)-anchor biosynthesis	3.349	10	Ribosome biogenesis in eukaryotes	2.333	10
	Fanconi anemia pathway	3.330	11	Fatty acid metabolism	2.280	11
	Dna replication	3.316	12	Nucleotide excision repair	2.170	12
	Pyrimidine metabolism	3.141	13	Pyrimidine metabolism	2.169	13
	Rna polymerase	3.021	14	Fatty acid degradation	2.160	14
	Mrna surveillance pathway	2.926	15	Rna degradation	2.157	15
	Endocytosis	2.840	16	Valine, leucine and isoleucine degradation	2.144	16
	Rna degradation	2.816	17	Biosynthesis of amino acids	2.140	17
	Mismatch repair	2.762	18	Glycosylphosphatidylinositol (gpi)-anchor biosynthesis	2.087	18
	Homologous recombination	2.747	19	Dna replication	2.066	19
	Peroxisome	2.699	20	Glycolysis / gluconeogenesis	2.065	20
Negative enrichment						
	Neuroactive ligand–receptor interaction	−2.490	1	Protein processing in endoplasmic reticulum	−3.896	1
	Wnt signaling pathway	−2.350	2	Endocytosis	−3.374	2
	Lysosome	−2.199	3	Spliceosome	−3.298	3
	Ecm-receptor interaction	−2.180	4	Wnt signaling pathway	−3.199	4
	Phagosome	−2.118	5	Ubiquitin mediated proteolysis	−2.849	5
	Mapk signaling pathway	−1.973	6	Tgf-beta signaling pathway	−2.782	6
	Calcium signaling pathway	−1.921	7	Mrna surveillance pathway	−2.738	7

(*continued on next page*)

Table 3 (*continued*)

Ag			SiO2		
Biological pathway	**NES**	**Rank**	**Biological pathway**	**NES**	**Rank**
Drug metabolism - cytochrome p450	−1.872	8	Mapk signaling pathway	−2.600	8
Autophagy - animal	−1.726	9	Calcium signaling pathway	−2.248	9
Age-rage signaling pathway in diabetic complications	−1.713	10	Ecm-receptor interaction	−2.077	10
Tgf-beta signaling pathway	−1.667	11	Phosphatidylinositol signaling system	−2.068	11
Glycosphingolipid biosynthesis - globo and isoglobo series	−1.593	12	Notch signaling pathway	−1.951	12
Erbb signaling pathway	−1.590	13	Autophagy - other	−1.946	13
Polyketide sugar unit biosynthesis	−1.589	14	Hippo signaling pathway -multiple species	−1.913	14
Taurine and hypotaurine metabolism*	−1.601	15	Autophagy - animal	−1.866	15
Glycosaminoglycan degradation*	−1.578	16	Inositol phosphate metabolism	−1.839	16
Autophagy - other*	−1.450	17	Neuroactive ligand–receptor interaction	−1.828	17
Hippo signaling pathway -multiple species*	−1.433	18	Phagosome	−1.816	18
Retinol metabolism*	−1.413	19	Mitophagy - animal	−1.804	19
Mitophagy - animal*	−1.376	20	Basal transcription factors	−1.700	20

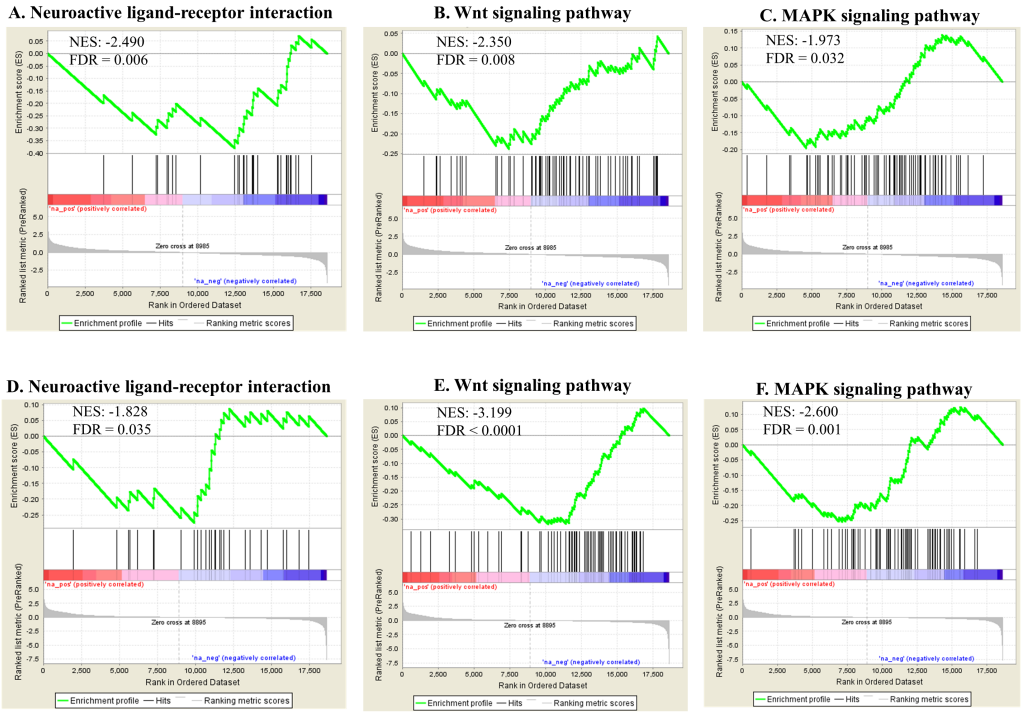

Figure 7 Selected significant KEGG pathways (detected by GSEA). Neuroactive ligand-receptor interaction, wnt signaling pathway and MAPK signaling pathway, negatively enriched based on NES, are shown in the Ag group (A–C) and the SiO2 group (D–F) (FDR < 0.05).

Full-size DOI: 10.7717/peerj.8684/fig-7

The top 20 significant KEGG pathways identified in both exposure studies are similar to the findings based on GO BPs. In particular, the regulatory biological pathways linked to phenotypes, including neuroactive ligand–receptor interaction (relates to locomotion Inoki et al., 2016), wnt and MAPK signaling pathways (relates to reproduction and cell growth (Inoki et al., 2016; *Hernandez Gifford, 2015*; *Zhang & Liu, 2002*; *Andrade et al., 2014*)), were found to be downregulated in both experiments. The pathway interaction analysis by ClueGO showed that wnt signaling pathway was interacting with tgf-beta pathway which was also enriched with significantly negative NES in both toxicities. These signaling pathways are known to interact with each other and control adult tissue homeostasis (*Warner, Greene & Pisano, 2005*). The downregulation of genes involved in neuroactive ligand receptor interaction likely to be responsible for the changes in locomotion.

The genes within the top 5 enriched gene category in the indicated pathways, commonly observed in both toxicities, were tachykinin receptor family (tkr-2), serotonin/octopamine receptor family (ser-1) (neuroactive ligand–receptor interaction pathway), skp1 related (ubiquitin ligase complex component, skr-8, skr-10, skr-12) (wnt signaling pathway), and protein ver-1 (ver-1) and heat shock protein (hsp 70) (MAPK signaling pathway). The proteins encoded by tachykinin receptor and ser-1 genes regulate locomotion via mediate neurotransmission and indirect modulation of neuromuscular circuits, respectively (*Pennefather, 2004*; *Dernovici et al., 2007*). The proteins encoded by skp1 related genes (such

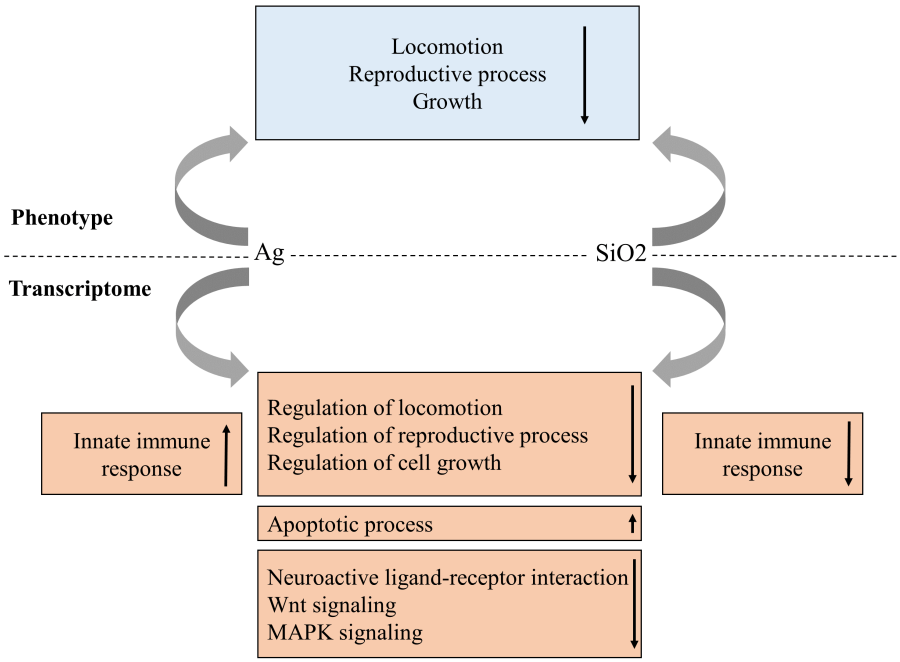

Figure 8 Proposed phenotype and transcriptome relationship in Ag and SiO2 toxicities. The gene enrichment profiles of the biological processes and pathways are concordant with phenotype characteristics for both toxicities. Arrows indicate gene enrichment profiles with negative or positive manner.
Full-size DOI: 10.7717/peerj.8684/fig-8

as skr-8 and skr-10) are known to be a core element of SCF ubiquitin-ligase complexes and involved in posterior body morphogenesis, embryonic and larval development, and cell proliferation in *C. elegans* (*Nayak et al., 2002*). Putative vascular endothelial growth factor receptors (VERs) of *C. elegans* and Hsp70 chaperones act in the PVF-1 signalling pathway for ray 1 positioning (in the male worms) and mediate protein folding, influencing various regulatory proteins, respectively (*Dalpe et al., 2013*; *Mayer & Bukau, 2005*). Overall, these genes may play significant roles on locomotion, reproduction and cell growth in response to nanotoxicity.

Apart from the many similarities observed between the two nanoparticle effects, Ag and SiO_2 also showed opposite effects on some of the top 20 enriched biological pathways. Spliceosome, mRNA surveillance and endocytosis pathways were enriched with positive NES in Ag, but with negative NES in SiO2, despite no obvious phenotypic differences were observed in our studies.

Comparison of the transcriptomics changes during Ag and SiO_2 exposures with the findings in previous studies on metal toxicities indicated that metallothionein-2 (mtl-2), a commonly observed responsive gene to the metal toxicities (conserved in *C. elegans* and mammals) (*Caito et al., 2012*; *Cui et al., 2007*; *Roh, Lee & Choi, 2006*; *Kumar et al., 2015*; *Anbalagan et al., 2012*), was up-regulated in these groups (FDR =0.002 for Ag, FDR = 0.043 for SiO2), which further confirmed the effectiveness of the model.

Ag and SiO_2nanoparticles have been shown to affect locomotion velocity in *C. elegans* N2, as previously described (*Jung et al., 2015*). In addition, Ag and SiO_2 have been shown

to reduce brood size, according to several studies (*Kleiven et al., 2018*; *Wu et al., 2013*; *Pluskota et al., 2009*). In contrast, we did not observe a significant decrease in brood size to exposure to 10 and 50 μg/ml of TiO_2 nanoparticles, as observed by *Wu et al. (2013)*, indicating differences in our conditions, as these authors saw a slight decrease in progeny production when using these nanoparticles in the μg/l concentration range. The effects of the other nanoparticles used in this study (i.e., CuO, Al_2O_3, and CeO_2) are relatively unknown based on the literature. In terms of neurotoxicity experiments, as determined by the number of head thrashes per minute in our study, our results differ from published results (*Wu et al., 2013*; *Pluskota et al., 2009*; *Piechulek & Von Mikecz, 2018*) which show that Ag and SiO_2 are neurotoxic at lower concentrations than the ones used in this study, although SiO_2 nanoparticles were found to have a modest effect at 50 μg/ml on neurotoxicity under our conditions. Indeed, we noticed that many neuron system-related BPs or pathways were enriched with negative NES in both Ag and SiO2 groups appear to have limited influence on head thrashing in our analysis. Additionally, our study is different compared to the indicated studies, as we only looked at the effect of nanoparticles incubated from the L1 stage to the adult day one stage. We observed that CeO_2, Al_2O_3 and CuO nanoparticles had significant neurotoxicity at 10 μg/ml, as determined by the decrease in number of head thrashes per minute, which is a novel observation. The reported differences in this study may be because the Ag and SiO_2 nanoparticles used in our study were confirmed to have a spherical shape under the manufacturer's test conditions (Table 1), whereas the others (TiO_2, CeO_2, Al_2O_3 and CuO) were unconfirmed to adopt any shape at all. Further study is required to elucidate the answer to this question. It was shown that co-feeding nanoparticles with *E. coli* OP50 in S-medium leads to the uptake of these nanoparticles through the pharynx and absorption through the gut (*Piechulek, Berwanger & Von Mikecz, 2019*). We speculate this to be true as well under our conditions. Silica (SiO_2) nanoparticles were shown to inhibit the peptide transporter OPT-2/PEP-2, present on the apical layer of the intestinal membrane in *C. elegans* (*Piechulek, Berwanger & Von Mikecz, 2019*). Inhibition of the OPT-2/PEP-2 transporter leads to the accumulation of silica nanoparticles in gut granules, indicating they are taken up within the organism. Fang-Yen et al. showed that particles with a diameter range of 0.5 μm to 3 μm are taken up by the pharynx (*Fang-Yen, Avery & Samuel, 2009*). We propose that this size range is circumvented when nanoparticles are co-fed with *E. coli* OP50 to gain access to the gut for absorption.

The observed effects in the various experiments can be either nanoparticle-specific or compound-/element-specific. Nanoparticles, ranging from 1 to 100 nm in size, are larger than their elemental constituents, which are metal cations under our experimental conditions. We reason that the observed effects in the various experiments and RNAseq analysis are due mainly to nanoparticles, although nanoparticles, such as Ag, release positively-charged ions upon incubation in liquid media and the proportion of released cations is small (*Lekamge et al., 2018*). In addition, metal oxide nanoparticles tend to release ions into liquid medium depending on the cationic metal charge (*Simeone & Costa, 2019*). For example, where Z is the oxidation number of the metal cation, oxides of nanoparticle cations with $Z \leq 2$ dissolve more than 10%, whereas this fraction is reduced to less than 1%

for nanoparticle oxides of cations with Z >3 (*Simeone & Costa, 2019*). According to this relationship, we would expect that less than 1% of the metal oxide nanoparticles used in our study to be dissolved, except for CuO nanoparticles which has a metal cation Z value of 2. As evidence for our reasoning, the WormExp enrichment analysis identified the "Ag NPs" term (Data S2).

To address whether the nanoparticles used in our study affected *E. coli* OP50 growth and thus C. elegans feeding, we incubated *E. coli* OP50 with 50 μg/ml of each nanoparticle in S-medium (Fig. S2). Compared to *E. coli* OP50 alone, the treated *E. coli* OP50, with the highest concentration of nanoparticles (50 μg/ml), demonstrated only slight growth defects, as determined by measuring bacterial density (Fig. S2). Antimicrobial nanoparticles, such as Ag nanoparticles, are antimicrobial as they interact with bacterial membranes and proteins through the released metal cations (*Sondi & Salopek-Sondi, 2004*). However, this effect seems to be minimal under our experimental conditions (Fig. S2), likely due to the low dissolution rate of Ag^{+} cations (*Lekamge et al., 2018*). Ag nanoparticles had only a major effect on bacterial density after five days compared to the other nanoparticles tested (Fig. S2). The same was observed for CuO nanoparticles (Fig. S2). Therefore, a constant source of *E. coli* OP50 food, as determined by bacterial density, was available during the course of the various experiments.

CONCLUSIONS

The aim of this study was to evaluate the effects of various nanoparticles on *C. elegans* using standard phenotyping assays and characterize transcriptomics changes of the worms exposed to selected nanoparticles (which showed the toxic effects for the majority of the parameters tested). With all these observations, we provide a novel angle to study the toxicity of nanoparticles on organisms, by exploring the mode of action of Ag and five metal oxide nanoparticles on different life history endpoints in *C. elegans*. To the best of our knowledge, this is the first study that integrates phenotype screening with RNAseq to investigate nanotoxicity in intact animals using *C. elegans*. Our RNAseq data not only confirmed positive enrichment of apoptotic process as reported in the literature (*McShan, Ray & Yu, 2014*; *Clement & Jarrett, 1994*; *Kim et al., 2015*), it also revealed that toxicities induced by both nanoparticles have down-regulated genes in multiple important regulatory biological processes and pathways, with opposite effects on innate immunity.

ADDITIONAL INFORMATION AND DECLARATIONS

Funding

This study was supported by the Fonds Québécois de la Recherche sur la Nature et les Technologies (FQRNT), Genome Canada, Genome Quebec and the Natural Sciences and Engineering Research Council of Canada (NSERC) Discovery Grant. The funders had no role in study design, data collection and analysis, decision to publish, or preparation of the manuscript.

Grant Disclosures

The following grant information was disclosed by the authors:
Fonds Québécois de la Recherche sur la Nature et les Technologies (FQRNT), Genome Canada, Genome Quebec.
The Natural Sciences and Engineering Research Council of Canada (NSERC) Discovery Grant.

Competing Interests

Jianguo Xia is an Academic Editor for PeerJ.

Author Contributions

- Charles Viau and Orçun Haçariz conceived and designed the experiments, performed the experiments, analyzed the data, prepared figures and/or tables, authored or reviewed drafts of the paper, and approved the final draft.
- Farial Karimian performed the experiments, prepared figures and/or tables, and approved the final draft.
- Jianguo Xia conceived and designed the experiments, authored or reviewed drafts of the paper, and approved the final draft.

Data Availability

The following information was supplied regarding data availability:

The raw data for Figs. 1–4 and Fig. S2 are available in the Supplemental Files. The RNAseq dataset is available in the NCBI Gene Expression Omnibus (GEO) database: GSE122728.

Supplemental Information

Supplemental information for this article can be found online at http://dx.doi.org/10.7717/peerj.8684#supplemental-information.

REFERENCES

Alsaleh NB, Brown JM. 2018. Immune responses to engineered nanomaterials: current understanding and challenges. *Current Opinion in Toxicology* **10**:8–14 DOI 10.1016/j.cotox.2017.11.011.

Anbalagan C, Lafayette I, Antoniou-Kourounioti M, Haque M, King J, Johnsen B, Baillie D, Gutierrez C, Martin JA, De Pomerai D. 2012. Transgenic nematodes as biosensors for metal stress in soil pore water samples. *Ecotoxicology* **21(2)**:439–455 DOI 10.1007/s10646-011-0804-0.

Anders S, Pyl PT, Huber W. 2015. HTSeq—a Python framework to work with high-throughput sequencing data. *Bioinformatics* **31(2)**:166–169 DOI 10.1093/bioinformatics/btu638.

Andrade LF, Mourão Mde M, Geraldo JA, Coelho FS, Silva LL, Neves RH, Volpini A, Machado-Silva JR, Araujo N, Nacif-Pimenta R, Caffrey CR, Oliveira G. 2014.

Regulation of Schistosoma mansoni development and reproduction by the mitogen-activated protein kinase signaling pathway. *PLOS Neglected Tropical Diseases* **8(6)**:e2949 DOI 10.1371/journal.pntd.0002949.

Bertani G. 1951. Studies on lysogenesis. I. The mode of phage liberation by lysogenic *Escherichia coli*. *Journal of Bacteriology* **62**:293–300 DOI 10.1128/JB.62.3.293-300.1951.

Bianchi L, Kwok SM, Driscoll M, Sesti F. 2003. A potassium channel-MiRP complex controls neurosensory function in *Caenorhabditis elegans*. *The Journal of Biological Chemistry* **278(14)**:12415–12424 DOI 10.1074/jbc.M212788200.

Bindea G, Mlecnik B, Hackl H, Charoentong P, Tosolini M, Kirilovsky A, Fridman WH, Pagès F, Trajanoski Z, Galon J. 2009. ClueGO: a cytoscape plug-in to decipher functionally grouped gene ontology and pathway annotation networks. *Bioinformatics* **25(8)**:1091–1093 DOI 10.1093/bioinformatics/btp101.

Boraschi D, Italiani P, Palomba R, Decuzzi P, Duschl A, Fadeel B, Moghimi SM. 2017. Nanoparticles and innate immunity: new perspectives on host defence. *Seminars in Immunology* **34**:33–51 DOI 10.1016/j.smim.2017.08.013.

Brenner S. 1974. The genetics of *Caenorhabditis elegans*. *Genetics* **77(1)**:71–94.

Caito S, Fretham S, Martinez-Finley E, Chakraborty S, Avila D, Chen P, Aschner M. 2012. Genome-wide analyses of metal responsive genes in *Caenorhabditis elegans*. *Frontiers in Genetics* **3**:52 DOI 10.3389/fgene.2012.00052.

Capco DG, Chen Y (eds.) 2014. *Nanomaterial impacts on cell biology and medicine*. Vol. 811. Dordrecht: Springer DOI 10.1007/978-94-017-8739-0.

Carlson M. 2018. org.Ce.eg.db: genome wide annotation for worm. R package version 3.6.0. *Available at https://bioconductor.org/packages/release/data/annotation/html/org.Ce.eg.db.html*.

Clement JL, Jarrett PS. 1994. Antibacterial silver. *Metal-Based Drugs* **1(5–6)**:467–482 DOI 10.1155/MBD.1994.467.

Cui Y, McBride SJ, Boyd WA, Alper S, Freedman JH. 2007. Toxicogenomic analysis of *Caenorhabditis elegans* reveals novel genes and pathways involved in the resistance to cadmium toxicity. *Genome Biology* **8(6)**:R122 DOI 10.1186/gb-2007-8-6-r122.

Dalpe G, Tarsitano M, Persico MG, Zheng H, Culotti J. 2013. *C. elegans* PVF-1 inhibits permissive UNC-40 signalling through CED-10 GTPase to position the male ray 1 sensillum. *Development* **140(19)**:4020–4030 DOI 10.1242/dev.095190.

Dekkers S, Krystek P, Peters RJ, Lankveld DP, Bokkers BG, Van Hoeven-Arentzen PH, Bouwmeester H, Oomen AG. 2011. Presence and risks of nanosilica in food products. *Nanotoxicology* **5(3)**:393–405 DOI 10.3109/17435390.2010.519836.

Dernovici S, Starc T, Dent JA, Ribeiro P. 2007. The serotonin receptor SER-1 (5HT2ce) contributes to the regulation of locomotion in *Caenorhabditis elegans*. *Developmental Neurobiology* **67(2)**:189–204 DOI 10.1002/dneu.20340.

Djurišić AB, Leung YH, Ng AM, Xu XY, Lee PK, Degger N, Wu RS. 2015. Toxicity of metal oxide nanoparticles: mechanisms, characterization, and avoiding experimental artefacts. *Small* **11(1)**:26–44 DOI 10.1002/smll.201303947.

Fang-Yen C, Avery L, Samuel ADT. 2009. Two size-selective mechanisms specifically trap bacteria-sized food particles in *Caenorhabditis elegans*. *Proceedings of the*

National Academy of Sciences of the United States of America **106(47)**:20093–20096 DOI 10.1073/pnas.0904036106.

Fröhlich E, Roblegg E. 2016. Oral uptake of nanoparticles: human relevance and the role of in vitro systems. *Archives of Toxicology* **90(10)**:2297–2314 DOI 10.1007/s00204-016-1765-0.

Gao J, Wang Y, Hovsepyan A, Bonzongo JC. 2011. Effects of engineered nanomaterials on microbial catalyzed biogeochemical processes in sediments. *Journal of Hazardous Materials* **186(1)**:940–945 DOI 10.1016/j.jhazmat.2010.11.084.

Gracida X, Eckmann CR. 2013. Fertility and germline stem cell maintenance under different diets requires nhr-114/HNF4 in *C. elegans*. *Current Biology* **23(7)**:607–613 DOI 10.1016/j.cub.2013.02.034.

Hernandez Gifford JA. 2015. The role of WNT signaling in adult ovarian folliculogenesis. *Reproduction* **150(4)**:R137–R148 DOI 10.1530/REP-14-0685.

Inoki K, Ouyang H, Zhu T, Lindvall C, Wang Y, Zhang X, Yang Q, Bennett C, Harada Y, Stankunas K, Wang CY, He X, MacDougald OA, You M, Williams BO, Guan KL. 2006. TSC2 integrates Wnt and energy signals via a coordinated phosphorylation by AMPK and GSK3 to regulate cell growth. *Cell* **126(5)**:955–968 DOI 10.1016/j.cell.2006.06.055.

Jung SK, Qu X, Aleman-Meza B, Wang T, Riepe C, Liu Z, Li Q, Zhong W. 2015. Multi-endpoint, high-throughput study of nanomaterial toxicity in *Caenorhabditis elegans*. *Environmental Science & Technology* **49(4)**:2477–2485 DOI 10.1021/es5056462.

Kaletta T, Hengartner MO. 2006. Finding function in novel targets: *C. elegans* as a model organism. *Nature Reviews. Drug Discovery* **5(5)**:387–398 DOI 10.1038/nrd2031.

Khanna P, Ong C, Bay BH, Baeg GH. 2015. Nanotoxicity: an interplay of oxidative stress, inflammation and cell death. *Nanomaterials* **5(3)**:1163–1180 DOI 10.3390/nano5031163.

Kim D, Langmead B, Salzberg SL. 2015. HISAT: a fast spliced aligner with low memory requirements. *Nature Methods* **12(4)**:357–360 DOI 10.1038/nmeth.3317.

Kim IY, Joachim E, Choi H, Kim K. 2015. Toxicity of silica nanoparticles depends on size, dose, and cell type. *Nanomedicine* **11(16)**:1407–1416 DOI 10.1016/j.nano.2015.03.004.

Kleiven M, Rossbach LM, Gallego-Urrea JA, Brede DA, Oughton DH, Coutris C. 2018. Characterizing the behavior, uptake, and toxicity of NM300K silver nanoparticles in *Caenorhabditis elegans*. *Environmental Toxicology and Chemistry* **37(7)**:1799–1810 DOI 10.1002/etc.4144.

Klopfenstein DV, Zhang L, Pedersen BS, Ramírez F, Warwick Vesztrocy A, Naldi A, Mungall CJ, Yunes JM, Botvinnik O, Weigel M, Dampier W, Dessimoz C, Flick P, Tang H. 2018. GOATOOLS: a Python library for gene ontology analyses. *Scientific Reports* **8(1)**:10872 DOI 10.1038/s41598-018-28948-z.

Knutson AK, Egelhofer T, Rechtsteiner A, Strome S. 2017. Germ granules prevent accumulation of somatic transcripts in the adult *Caenorhabditis elegans* Germline. *Genetics* **206(1)**:163–178 DOI 10.1534/genetics.116.198549.

Komatsu H, Mori I, Rhee JS, Akaike N, Ohshima Y. 1996. Mutations in a cyclic nucleotide-gated channel lead to abnormal thermosensation and chemosensation in *C. elegans*. *Neuron* **17(4)**:707–718 DOI 10.1016/S0896-6273(00)80202-0.

Kong Y, Liang X, Liu L, Zhang D, Wan C, Gan Z, Yuan L. 2015. High throughput sequencing identifies MicroRNAs mediating α-synuclein toxicity by targeting neuroactive-ligand receptor interaction pathway in early stage of drosophila parkinson's disease model. *PLOS ONE* **10(9)**:e0137432 DOI 10.1371/journal.pone.0137432.

Kumar R, Pradhan A, Khan FA, Lindström P, Ragnvaldsson D, Ivarsson P, Olsson PE, Jass J. 2015. Comparative analysis of stress induced gene expression in caenorhabditis elegans following exposure to environmental and lab reconstituted complex metal mixture. *PLOS ONE* **10(7)**:e0132896 DOI 10.1371/journal.pone.0132896.

Lekamge S, Miranda AF, Abraham A, Li V, Shukla R, Bansal V, Nugegoda D. 2018. The toxicity of silver nanoparticles (AgNPs) to three freshwater invertebrates with different life strategies: *Hydra vulgaris*, *Daphnia carinata*, and *Paratya australiensis*. *Frontiers in Environmental Science* **6**:152 DOI 10.3389/fenvs.2018.00152.

Lewis JA, Fleming JT. 1995. Basic culture methods. *Methods in Cell Biology* **48**:3–29 DOI 10.1016/S0091-679X(08)61381-3.

Li H, Handsaker B, Wysoker A, Fennell T, Ruan J, Homer N, Marth G, Abecasis G, Durbin R, 1000 Genome Project Data Processing Subgroup. 2009. The sequence alignment/map format and SAMtools. *Bioinformatics* **25(16)**:2078–2079 DOI 10.1093/bioinformatics/btp352.

Luo W, Friedman MS, Shedden K, Hankenson KD, Woolf PJ. 2009. GAGE: generally applicable gene set enrichment for pathway analysis. *BMC Bioinformatics* **10**:161 DOI 10.1186/1471-2105-10-161.

Mayer MP, Bukau B. 2005. Hsp70 chaperones: cellular functions and molecular mechanism. *Cellular and Molecular Life Sciences* **62(6)**:670–684 DOI 10.1007/s00018-004-4464-6.

Mayer S, Raulf MK, Lepenies B. 2017. C-type lectins: their network and roles in pathogen recognition and immunity. *Histochemistry and Cell Biology* **147(2)**:223–237 DOI 10.1007/s00418-016-1523-7.

Maynard AD. 2011. Don't define nanomaterials. *Nature* **475(7354)**:31–31 DOI 10.1038/475031a.

McShan D, Ray PC, Yu H. 2014. Molecular toxicity mechanism of nanosilver. *Journal of Food and Drug Analysis* **22(1)**:116–127 DOI 10.1016/j.jfda.2014.01.010.

Medina C, Santos-Martinez MJ, Radomski A, Corrigan OI, Radomski MW. 2007. Nanoparticles: pharmacological and toxicological significance. *British Journal of Pharmacology* **150(5)**:552–558 DOI 10.1038/sj.bjp.0707130.

National Research Council. 2000. *Scientific frontiers in developmental toxicology and risk assessment*. Washington, D.C.: Committee on Developmental Toxicology, Board on Environmental Studies and Toxicology. National Academies Press (US). National Academy of Sciences.

Nayak S, Santiago FE, Jin H, Lin D, Schedl T, Kipreos ET. 2002. The *Caenorhabditis elegans* Skp1-related gene family: diverse functions in cell proliferation, morphogenesis, and meiosis. *Current Biology* **12(4)**:277–287 DOI 10.1016/S0960-9822(02)00682-6.

Oberdörster G. 2010. Safety assessment for nanotechnology and nanomedicine: concepts of Nanotoxicology. *Journal of Internal Medicine* **267(1)**:89–105 DOI 10.1111/j.1365-2796.2009.02187.x.

Pennefather JN. 2004. Tachykinins and tachykinin receptors: a growing family. *Life Sciences* **74(12)**:1445–1463 DOI 10.1016/j.lfs.2003.09.039.

Piechulek AA, Berwanger LC, Von Mikecz P. 2019. Silica nanoparticles disrupt OPT-2/PEP-2-dependent trafficking of nutrient peptides in the intestinal epithelium. *Nanotoxicology* **13(8)**:1133–1148 DOI 10.1080/17435390.2019.1643048.

Piechulek AA, Von Mikecz A. 2018. Life span-resolved nanotoxicology enables identification of age-associated neuromuscular vulnerabilities in the nematode *Caenorhabditis elegans*. *Environmental Pollution* **233**:1095–1103 DOI 10.1016/j.envpol.2017.10.012.

Pluskota A, Horzowski E, Bossinger O, Von Mikecz A. 2009. In *Caenorhabditis elegans* nanoparticle-bio-interactions become transparent: silica-nanoparticles induce reproductive senescence. *PLOS ONE* **4(8)**:e6622 DOI 10.1371/journal.pone.0006622.

Powell JA. 2014. GO2MSIG, an automated GO based multi-species gene set generator for gene set enrichment analysis. *BMC Bioinformatics* **15**:146 DOI 10.1186/1471-2105-15-146.

Robinson MD, McCarthy DJ, Smyth GK. 2010. edgeR: a bioconductor package for differential expression analysis of digital gene expression data. *Bioinformatics* **26(1)**:139–140 DOI 10.1093/bioinformatics/btp616.

Rocheleau S, Arbour M, Elias M, Sunahara GI, Masson L. 2015. Toxicogenomic effects of nano- and bulk-TiO2 particles in the soil nematode *Caenorhabditis elegans*. *Nanotoxicology* **9(4)**:502–512 DOI 10.3109/17435390.2014.948941.

Roh JY, Lee J, Choi J. 2006. Assessment of stress-related gene expression in the heavy metal-exposed nematode *Caenorhabditis elegans*: a potential biomarker for metal-induced toxicity monitoring and environmental risk assessment. *Environmental Toxicology and Chemistry* **25(11)**:2946–2956 DOI 10.1897/05-676r.1.

Roubin R, Naert K, Popovici C, Vatcher G, Coulier F, Thierry-Mieg J, Pontarotti P, Birnbaum D, Baillie D, Thierry-Mieg D. 1999. let-756, a *C. elegans* fgf essential for worm development. *Oncogene* **18(48)**:6741–6747 DOI 10.1038/sj.onc.1203074.

Ruiz-Lancheros E, Viau C, Walter TN, Francis A, Geary TG. 2011. Activity of novel nicotinic anthelmintics in cut preparations of *Caenorhabditis elegans*. *International Journal for Parasitology* **41(3–4)**:455–461 DOI 10.1016/j.ijpara.2010.11.009.

Scharf A, Gührs KH, Von Mikecz A. 2016. Anti-amyloid compounds protect from silica nanoparticle-induced neurotoxicity in the nematode *C. elegans*. *Nanotoxicology* **10(4)**:426–435 DOI 10.3109/17435390.2015.1073399.

Scheel J, Srinivasan J, Honnert U, Henske A, Kurzchalia TV. 1999. Involvement of caveolin-1 in meiotic cell-cycle progression in *Caenorhabditis elegans*. *Nature Cell Biology* **1(2)**:127–129 DOI 10.1038/10100.

Shannahan J. 2017. The biocorona: a challenge for the biomedical application of nanoparticles. *Nanotechnology Reviews* **6(4)**:345–353 DOI 10.1515/ntrev-2016-0098.

Simeone FC, Costa AL. 2019. Assessment of cytotoxicity of metal oxide nanoparticles on the basis of fundamental physical–chemical parameters: a robust approach to grouping. *Environmental Science: Nano* **6**:3102–3112 DOI 10.1039/c9en00785g.

Sondi I, Salopek-Sondi B. 2004. Silver nanoparticles as antimicrobial agent: a case study on *E. coli* as a model for Gram-negative bacteria. *Journal of Colloid and Interface Science* **275(1)**:177–182 DOI 10.1016/j.jcis.2004.02.012.

Sonowal R, Swimm A, Sahoo A, Luo L, Matsunaga Y, Wu Z, Bhingarde JA, Ejzak EA, Ranawade A, Qadota H, Powell DN, Capaldo CT, Flacker JM, Jones RM, Benian GM, Kalman D. 2017. Indoles from commensal bacteria extend healthspan. *Proceedings of the National Academy of Sciences of the United States of America* **114(36)**:E7506–E7515 DOI 10.1073/pnas.1706464114.

Staab TA, Griffen TC, Corcoran C, Evgrafov O, Knowles JA, Sieburth D. 2013. The conserved SKN-1/Nrf2 stress response pathway regulates synaptic function in *Caenorhabditis elegans*. *PLOS Genetics* **9(3)**:e1003354 DOI 10.1371/journal.pgen.1003354.

Starnes DL, Lichtenberg SS, Unrine JM, Starnes CP, Oostveen EK, Lowry GV, Bertsch PM, Tsyusko OV. 2016. Distinct transcriptomic responses of Caenorhabditis elegans to pristine and sulfidized silver nanoparticles. *Environmental Pollution* **213**:314–321 DOI 10.1016/j.envpol.2016.01.020.

Stiernagle T. 2006. Maintenance of *C. elegans*. *WormBook* **2006**:1–11 DOI 10.1895/wormbook.1.101.1.

Subramanian A, Tamayo P, Mootha VK, Mukherjee S, Ebert BL, Gillette MA, Paulovich A, Pomeroy SL, Golub TR, Lander ES, Mesirov JP. 2005. Gene set enrichment analysis: a knowledge-based approach for interpreting genome-wide expression profiles. *Proceedings of the National Academy of Sciences of the United States of America* **102(43)**:15545–15550 DOI 10.1073/pnas.0506580102.

Sulston J, Hodgkin J. 1988. Methods. In: Wood WB, ed. *The nematode Caenorhabditis elegans*. Plainview: Cold Spring Harbor Laboratory Press, 587–606.

Tsalik EL, Hobert O. 2003. Functional mapping of neurons that control locomotory behavior in *Caenorhabditis elegans*. *Journal of Neurobiology* **56(2)**:178–197 DOI 10.1002/neu.10245.

Uchida O, Nakano H, Koga M, Ohshima Y. 2003. The *C. elegans* che-1 gene encodes a zinc finger transcription factor required for specification of the ASE chemosensory neurons. *Development* **130(7)**:1215–1224 DOI 10.1242/dev.00341.

Warner DR, Greene RM, Pisano MM. 2005. Cross-talk between the TGFbeta and Wnt signaling pathways in murine embryonic maxillary mesenchymal cells. *FEBS Letters* **579(17)**:3539–3546 DOI 10.1016/j.febslet.2005.05.024.

Wu Q, Nouara A, Li Y, Zhang M, Wang W, Tang M, Ye B, Ding J, Wang D. 2013. Comparison of toxicities from three metal oxide nanoparticles at environmental relevant concentrations in nematode *Caenorhabditis elegans*. *Chemosphere* **90(3)**:1123–1131 DOI 10.1016/j.chemosphere.2012.09.019X.

Yang W, Dierking K, Schulenburg H. 2016. WormExp: a web-based application for a *Caenorhabditis elegans*-specific gene expression enrichment analysis. *Bioinformatics* **32(6)**:943–945 DOI 10.1093/bioinformatics/btv667.

Zhang W, Liu HT. 2002. MAPK signal pathways in the regulation of cell proliferation in mammalian cells. *Cell Research* **12(1)**:9–18 DOI 10.1038/sj.cr.7290105.

Zhou G, Soufan O, Ewald J, Hancock REW, Basu N, Xia J. 2019. NetworkAnalyst 3.0: a visual analytics platform for comprehensive gene expression profiling and meta-analysis. *Nucleic Acids Research* **47(W1)**:W234–W241 DOI 10.1093/nar/gkz240.